

Copyright Warning & Restrictions

The copyright law of the United States (Title 17, United States Code) governs the making of photocopies or other reproductions of copyrighted material.

Under certain conditions specified in the law, libraries and archives are authorized to furnish a photocopy or other reproduction. One of these specified conditions is that the photocopy or reproduction is not to be “used for any purpose other than private study, scholarship, or research.” If a user makes a request for, or later uses, a photocopy or reproduction for purposes in excess of “fair use” that user may be liable for copyright infringement,

This institution reserves the right to refuse to accept a copying order if, in its judgment, fulfillment of the order would involve violation of copyright law.

Please Note: The author retains the copyright while the New Jersey Institute of Technology reserves the right to distribute this thesis or dissertation

Printing note: If you do not wish to print this page, then select “Pages from: first page # to: last page #” on the print dialog screen

The Van Houten library has removed some of the personal information and all signatures from the approval page and biographical sketches of theses and dissertations in order to protect the identity of NJIT graduates and faculty.

ABSTRACT

A Theoretical Model for Biased Superlattice Devices

by
Michael Ferner

A model describing the subband structures and tunneling characteristics of superlattices is presented. The model solves the envelope function equations by the transfer matrix technique. The results are codified in a Fortran program, and the model is applied to several structures.

Superlattice have been studied extensively, however many new structures await investigation.

This model is presented as a preliminary design tool. The program allows a designer to do preliminary calculations. This type of investigation guides a designer toward a goal by making possible a large number of calculations on many different structures.

A THEORETICAL MODEL FOR BIASED SUPERLATTICE DEVICES

by
Michael Ferner

A Thesis
Submitted to the Faculty of
New Jersey Institute of Technology
in Partial Fulfillment of the Requirements
for the Degree of Master of Science
Department of Applied Physics
December, 1992

APPROVAL PAGE
A THEORETICAL MODEL FOR BIASED
SUPERLATTICE DEVICES

by
Michael Ferner

Dr. K. Ken Chju, Thesis Advisor
Professor of Physics, NJIT

Dr. John C. Hensel, Committee Member
Distinguished Research Professor of Physics, NJIT

Dr. Vincent Santarelli, Committee Member
Associate Professor of Physics, Rutgers University

BIOGRAPHICAL SKETCH

Author: Michael Ferner

Degree: Master of Science in Applied Physics

Date: December, 1992

Undergraduate and Graduate Education:

Master of Science in Applied Physics
New Jersey Institute of Technology, Newark, NJ, 1992

Bachelor of Arts in Physics and Mathematics
Rutgers University of New Jersey, Newark, NJ, 1989

Major: Applied Physics

This thesis is dedicated to
Ludy A. Verbo

ACKNOWLEDGMENT

The author wishes to thank Dr. K. Ken Chin, his thesis advisor. Dr. Chin has provided guidance and has shown a genuine interest in this author's graduate studies.

The author thanks Hong Chen for laying the foundation upon which this work rests. Mr. Chen's work is a significant achievement and is cited in this work. The discussions the author had with Mr. Chen were enlightening and helpful.

Also, thanks are due Dr. Hensel and Dr. Santarelli for serving as members of the committee.

The author is grateful to his family, friends, and colleagues for providing encouragement. Special thanks to Uncle Steve for typing the equations that appear throughout this work.

Finally, the author wishes to express his love and appreciation for his girlfriend, Ludy A. Verbo. She has been and continues to be a source of inspiration and assistance.

TABLE OF CONTENTS

Chapter	Page
1 INTRODUCTION	1
2 THE ENVELOPE FUNCTION APPROXIMATION	4
2.1 Kane's $k \cdot p$ Theory	4
2.2 Envelope Functions	6
3 TRANSFER MATRIX SOLUTION	8
3.1 Introduction	8
3.2 Transfer Matrix Solution	9
3.2.1 Basic Equation	9
3.2.2 Transfer Matrix for One Layer	11
3.2.3 Transfer Matrix for Multiple Layers	13
3.3 Tunneling	14
4 THE APPLIED BIAS VOLTAGE	19
4.1 Introduction	19
4.2 Biasing a Layered Dielectric	19
4.2.1 Statement of the Problem	19
4.2.2 Solution to the Problem	20
4.3 The Step Approximation	21
4.3.1 The Tilted Bands	21
4.3.2 The Step Approximation	23
4.4 The Fortran Program	24
5 APPLYING THE SUPERLATTICE MODEL TO A DESIGN GOAL	26
5.1 Introduction	26
5.2 General Considerations	27
5.3 Preliminary Structure	28
APPENDIX	34
A.1 Introduction	34
A.2 Input Files	35
A.3 Fortran-77 Program	37
A.4 Output Files	43
BIBLIOGRAPHY	45

LIST OF FIGURES

Figure	Page
3.1 A Multiple Layered Structure	13
3.2 Elementary Tunneling Model	14
4.1 Biased Dielectric Layers	20
4.2 Sample Band Structure	21
4.3 A Tilted Band	22
4.4 Steps Approximating a Tilted Band	23
5.1 Current Injection Scheme	27
5.2 Structure 1	28
5.3 Tunneling Data for Structure 1	29
5.4 Structure 2	30
5.5 Data for Structure 2	31
5.6 Structure 3	32
5.7 Data for Structure 3	33
A.1 Pictorial Representation of Computer Files	34
A.2 Sample Input File 'initial.dat;1' and Graphical Representation	35
A.3 Sample Input File 'slope.dat;1' and Graph of Step Approximation	36
A.4 Preliminary Graph Produced by Program	44

CHAPTER 1

INTRODUCTION

A useful and efficient model describing electronic subband structures and tunneling characteristics in multiple quantum wells (MQW) or superlattices is the topic of this thesis. Such a model provides a designer of such structures with a means of making preliminary decisions and calculations. Fine tuning a structure to better realize a particular phenomena and discovering a new device application are two purposes accomodated by a practical, superlattice model. The model discussed in this work culminates with a Fortran program included in the appendix.

Many superlattices have been grown and studied to date. In fact, ultrathin superlattices became widely studied because of advances in microstructure technology such as molecular beam epitaxy and electron beam lithography. However, unlike conventional semiconductor materials, superlattices provide a seemingly endless variety of structures to study. Material choices, band edge lineups, and layer thicknesses are among the parameters that can be varied by the designer. Needless to say, many new structures await investigation.

Having established that a theoretical model with computer code can be of value to a designer in the preliminary stages of development, it remains to discuss what matters must

be addressed by such a model. Consider that the energy band offsets between bands of superlattice layers are typically on the order of hundreds of meV. Since modifications to electronic structure that are due to the periodic "modulation" of the superlattice are on this scale, a useful theoretical model should deal with questions on this scale.

Furthermore, electronic states with mean free paths much smaller than a layer's thickness are essentially confined within that layer. On the other hand, states with mean free paths comparable to or greater than the thickness of layers are appreciably modulated by the periodic superlattice. Therefore, states of interest are close in energy to band edges with relatively long lifetimes and mean free paths. It is required, then, that the superlattice model be a band edge theory.

The theoretical scheme employed by this work is based on the envelope function approximation starting from Kane's $k \cdot p$ theory. This method focuses on the above mentioned "interesting states" and consolidates other facets of the superlattice into effective parameters. Chapter two deals with these matters. The resulting, Schrodinger-like equation, called the envelope function equation, is solved in chapter three by the transfer matrix technique. A difficulty arises when an applied bias voltage is considered. This problem of handling the bias potential is addressed in chapter four. Also, in chapter four, the Fortran program is discussed. Chapter five presents several structures and summarizes the information obtained

from the model. Finally, the computer program and sample input and output files are included in the appendix.

The intent of this work is to demonstrate the increasing role of computer simulation and computational methods in applied physics research. However, this author seeks to obtain analytic results from an appropriate theoretical model wherever possible. The computer code is written only to do the tedious calculations quickly. While there is no substitute for real experimentation, this model with computer code can be of great value in the preliminary stages of research.

CHAPTER 2

THE ENVELOPE FUNCTION APPROXIMATION

2.1 KANE'S $\mathbf{k} \cdot \mathbf{p}$ THEORY

Superlattices provide for a diverse collection of phenomena^[3]. The theory one adopts to explain a particular effect depends on what superlattice application one has in mind. In bulk semiconductors, $\mathbf{k} \cdot \mathbf{p}_{\text{op}}$ theory effectively describes states near band edges. As was mentioned in chapter one, it is these band edge states that are of interest when discussing superlattices. It is reasonable, then, to apply this theory to superlattices.

The $\mathbf{k} \cdot \mathbf{p}_{\text{op}}$ representation comes from the Schrodinger Equation.

$$\left\{ \frac{P_{\text{op}}^2}{2\mu} + V \right\} \psi = E \psi \quad (2.1)$$

Bloch showed that the solution of eq(2.1) can be written in terms of eigenfunctions $\Psi_{\mathbf{n}\mathbf{k}}$, with \mathbf{k} in the first Brillouin zone and \mathbf{n} indexing the electron's energy bands.

$$\psi_{n\mathbf{k}}(\mathbf{r}) = U_{n\mathbf{k}}(\mathbf{r}) e^{i(\mathbf{k}\cdot\mathbf{r})} \quad (2.2)$$

In eq(2.2) $U_{n\mathbf{k}}(\mathbf{r})$ has the periodicity of $V(\mathbf{r})$ and the exponential factor describes a free electron plane wave with momentum $\hbar\mathbf{k}$. The infinite set of $U_{n\mathbf{k}}(\mathbf{r})$ form a complete set for a given \mathbf{k} , say \mathbf{k}_0 . For a different \mathbf{k} we have the so called \mathbf{k}_0 representation. Eq(2.3) means that any function with the periodicity of $V(\mathbf{r})$ can be expressed in terms of the infinite basis, the $U_{n\mathbf{k}}(\mathbf{r})$.

$$U_{n\mathbf{k}}(\mathbf{r}) = \sum_m C_{nm}(\mathbf{k} - \mathbf{k}_0) U_{m\mathbf{k}_0}(\mathbf{r}) \quad (2.3)$$

The theory continues to get a matrix eigen-value equation that can be treated by perturbation theory. The details are not included here. A previous thesis[31] derives and solves this matrix equation using Kane's model.

Kane's model[1,8] deals with the perturbation term. For Zincblende III-V and II-VI materials, the fundamental band gap occurs at $\mathbf{k}_0=0$. The infinite series, eq(2.3) is truncated to eight terms near the fundamental band gap. Four terms in the conduction band and four terms in the valence band are used to approximate the infinite series.

2.2 ENVELOPE FUNCTIONS

The envelope function method[4-10] is essentially a plane wave model. The envelope function is built as a sum of products of slowly varying functions on the scale of the host unit cell. Rapidly varying functions are consolidated into effective parameters. The host crystalline potentials, the fixed band gap, and the effective masses of the host materials are considered known. The goal is to find a Schrodinger-like equation governing the states that are considered interesting. The derivation of such an equation is not included here. The derivation is included in Chen's work[31]. The equation, called the envelope function equation will be solved in chapter three and is included here as equation 2.4

$$\left\{ P_z \frac{1}{2\mu} P_z + V_s(z) + V_{\text{ext}}(z) \right\} f = E f \quad (2.4a)$$

$$f \quad \text{and} \quad \frac{1}{\mu} \frac{df}{dz} \quad \text{are continuous} \quad (2.4b)$$

In eq(2.4a), f is the envelope function. It is the wave function describing the large scale, interesting states discussed previously. E is energy. The operator P_z is given by eq(2.5).

$$P_z = \frac{\hbar}{i} \frac{d}{dz} \quad (2.5)$$

The effective mass μ is different for each layer and depends on energy and position. V_s is the conduction band offset related to the first layer, and V_{ext} is the external potential.

The boundary conditions given by eq(2.4b) apply at the boundaries between layers of the superlattice. Additional boundary conditions called the Born - von Karman expansion are built into the formalism. Only a finite number of layers can be studied so it is required that the last layer be the same as the first.

CHAPTER 3 TRANSFER MATRIX SOLUTION

3.1 INTRODUCTION

At this point, a Schrodinger-like equation exists and needs to be solved. This equation, the envelope function equation, will yield all required information about electronic structure and transport properties of a given MQW device. The characteristics of the host materials are included as effective parameters to make possible this analytic solution, called the transfer matrix solution.

The method constructs a transfer matrix for each layer of a period of a MQW. This transfer matrix is formed by the solution of the envelope function equation, and it depends on the structural and band parameters of a given layer. The transfer matrix of more than one layer is the matrix product of matrices of the constituent layers. This chapter will outline the formalism and show that the transfer matrix of a period of a device is the required solution.

This chapter is organized into three sections following this introduction. First, the formalism is discussed, leading to the above mentioned solution. Secondly, tunneling is discussed. Finally, the subband structure for a MQW is briefly described.

3.2 TRANSFER MATRIX SOLUTION

3.2.1 Basic Equation

In the previous chapter, the envelope function equation was obtained and is written here as eqs.(3.1) and (3.2).

$$\left[\left(P_z \right) \left(\frac{1}{2\mu(E, Z)} P_z \right) + V_s(Z) + V_{ext}(Z) \right] \hat{f} = E \hat{f} \quad (3.1)$$

$$f \text{ and } \frac{1}{\mu} \frac{df}{dz} \text{ are continuous everywhere} \quad (3.2)$$

These equations appeared as eqs(2.4) and the description of the variables in the above equations is given in section 2.2.

To begin, define the state vector

$$\hat{f}(Z) = \begin{bmatrix} F_a(Z) \\ F_b(Z) \end{bmatrix} = \begin{bmatrix} f \\ \frac{1}{\mu} \frac{df}{dZ} \end{bmatrix} \quad (3.3)$$

with continuous components that satisfy equation 3.2. It is easily verified that the components of \hat{f} satisfy the coupled eqs.(3.4) and are consistent with eq.(3.1).

$$F'_a = \mu F_b \quad (3.4a)$$

$$F'_b = - \left[\frac{2(E - V_s - V_{ext})}{\hbar^2} \right] F_a \quad (3.4b)$$

In matrix form this can be written as

$$\begin{bmatrix} F'_a \\ F'_b \end{bmatrix} = \begin{bmatrix} 0 & \mu \\ -\frac{k^2}{\mu} & 0 \end{bmatrix} \begin{bmatrix} F_a \\ F_b \end{bmatrix} \quad (3.5a)$$

where

$$k^2 = \frac{2\mu(E - V_s - V_{ext})}{\hbar^2} \quad (3.5b)$$

Eqs.(3.5) are the basic equations to be solved. Many techniques exist to solve eqs(3.5). The results are eqs(3.6).

$$F_a(z) = F_{a0} \cos(kz) + \frac{\mu}{k} F_{b0} \sin(kz) \quad (3.6a)$$

$$F_b(z) = -\frac{k}{\mu} F_{b0} \sin(kz) + F_{b0} \cos(kz) \quad (3.6b)$$

In the development to follow, the solution sets that will be used satisfy certain initial conditions and are given as eqs(3.7).

$$f^{(1)}(z) = \begin{pmatrix} \cos(kz) \\ -\frac{k}{\mu} \sin(kz) \end{pmatrix}, \quad f^{(1)}(0) = \begin{pmatrix} 1 \\ 0 \end{pmatrix} \quad (3.7a)$$

$$f^{(2)}(z) = \begin{pmatrix} \frac{\mu}{k} \sin(kz) \\ \cos(kz) \end{pmatrix}, \quad f^{(2)}(0) = \begin{pmatrix} 0 \\ 1 \end{pmatrix} \quad (3.7b)$$

3.2.2 Transfer Matrix for One Layer

It can be shown^[30] that f satisfies

$$f(z_1) = S(z_1, z_2) \cdot f(z_2) \quad (3.8)$$

where

$$S(Z_1, Z_2) = \begin{bmatrix} F_a^{(1)}(Z_1 - Z_2) & F_a^{(2)}(Z_1 - Z_2) \\ F_b^{(1)}(Z_1 - Z_2) & F_b^{(2)}(Z_1 - Z_2) \end{bmatrix} \quad (3.9)$$

The transfer matrix $S(z_1, z_2)$ has the properties (3.10).

$$\det \{S(Z_1, Z_2)\} = 1 \quad (3.10a)$$

$$S(Z_1, Z_2) = S^{-1}(Z_2, Z_1) \quad (3.10b)$$

$$S(Z_1, Z_2) \Big|_{z_1 = z_2} = I \quad (3.10c)$$

If μ and k are constant in the region between z_1 and z_2 , such as in a single superlattice layer, then the transfer matrix is given by eq(3.11).

$$S(Z_1, Z_2) = \begin{bmatrix} \cos(k(Z_1 - Z_2)) & \frac{\mu}{k} \sin(k(Z_1 - Z_2)) \\ -\frac{k}{\mu} \sin(k(Z_1 - Z_2)) & \cos(k(Z_1 - Z_2)) \end{bmatrix} \quad (3.11)$$

Essentially eq(3.11) is the transfer matrix for one layer of a MQW. For example, if the layer has a thickness L , then the state $f(L)$ can be found by $f(L) = S(L, 0) f(0)$ provided the state $f(0)$ is known.

3.2.3 Transfer Matrix for Multiple Layers

Consider a multiple layered structure such as figure 3.1.

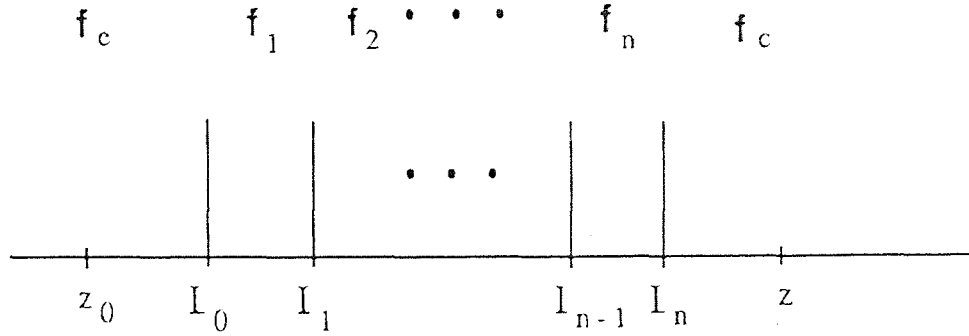


Figure 3.1 A Multiple Layered Structure

Within the i^{th} layer $f_i(L_i) = S(L_i, L_{i-1}) \cdot f_i(L_{i-1})$, and at the boundaries f is continuous so that $f_i(L_i) = f_{i+1}(L_i)$. Clearly, the process of induction yields the following:

$$\begin{aligned}
 f_c(z) &= S_c(z, L_n) f_n(L_n) \\
 &= S_c(z, L_n) S_c(L_n, L_{n-1}) f_{n-1}(L_{n-1}) \\
 &\quad \Downarrow \\
 &= S_c(z, L_n) S(L_n, L_0) S_0(L_0, z_0) f_c(z_0)
 \end{aligned}$$

This leads to the result eq(3.12)

$$S(L_n, L_0) = \prod S_i(L_i, L_{i-1}) \quad \text{for } i=n, \dots, 1 \quad (3.12)$$

S is the transfer matrix of the N -layered structure, and it is the simple matrix product of transfer matrices of the form given by eq(3.11)

3.3 TUNNELING

To calculate the tunneling coefficient T_{tunnel} , consider an incident plane wave with unit amplitude striking a layered structure shown in figure 3.2. The wave is partially transmitted and reflected with amplitudes T and R respectively. The wave functions are:

$$f_e(z) = e^{ik_e z} + R e^{-ik_e z} \quad \text{for } z < 0 \quad (3.13a)$$

$$f_c(z) = T e^{ik_c z} \quad \text{for } z > L \quad (3.13b)$$

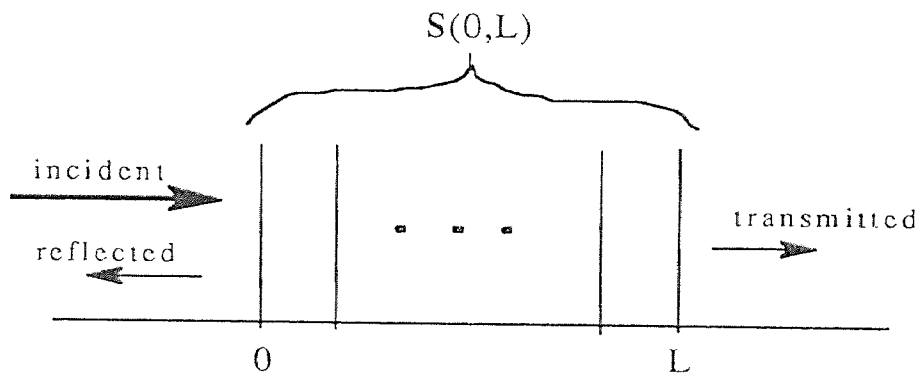


Figure 3.2 Elementary Tunneling Model

The corresponding state vectors are given in a general form as eqs(3.14).

$$\mathbf{f}_e(Z) = \begin{bmatrix} 1 & 1 \\ \frac{ik_e}{\mu_e} & -\frac{ik_e}{\mu_e} \end{bmatrix} \begin{pmatrix} e^{ik_e Z} \\ R e^{-ik_e Z} \end{pmatrix} \quad (3.14a)$$

$$\mathbf{f}_c(Z) = \begin{bmatrix} 1 & 1 \\ \frac{ik_c}{\mu_c} & -\frac{ik_c}{\mu_c} \end{bmatrix} \begin{pmatrix} T e^{ik_c Z} \\ 0 \end{pmatrix} \quad (3.14b)$$

Now, the tunneling coefficient is defined as

$$T_{\text{tunnel}} = \frac{k_c \mu_e}{k_e \mu_c} |T|^2 \quad (3.15)$$

It remains to solve for T_{tunnel} in terms of the transfer matrix. The following equations show the details of the calculation.

$$\mathbf{f}_c(L) = \mathbf{S}(L, 0) \mathbf{f}_e(0)$$

$$\begin{bmatrix} 1 & 1 \\ \frac{ik_c}{\mu_c} & -\frac{ik_c}{\mu_c} \end{bmatrix} \begin{pmatrix} T e^{ik_c L} \\ 0 \end{pmatrix} = \mathbf{S}(L, 0) \begin{bmatrix} 1 & 1 \\ \frac{ik_e}{\mu_e} & -\frac{ik_e}{\mu_e} \end{bmatrix} \begin{pmatrix} 1 \\ R \end{pmatrix}$$

$$\begin{aligned}
\begin{pmatrix} T e^{ik_c L} \\ 0 \end{pmatrix} &= \frac{1}{2} \begin{bmatrix} 1 & \frac{\mu_c}{ik_c} \\ 1 & \frac{-\mu_c}{ik_c} \end{bmatrix} \cdot S(L, 0) \cdot \begin{bmatrix} 1 & 1 \\ \frac{ik_e}{\mu_e} & \frac{-ik_e}{\mu_e} \end{bmatrix} \begin{pmatrix} 1 \\ R \end{pmatrix} \\
&= M \begin{pmatrix} 1 \\ R \end{pmatrix} = \begin{bmatrix} M_{11} & M_{12} \\ M_{21} & M_{22} \end{bmatrix} \begin{pmatrix} 1 \\ R \end{pmatrix}
\end{aligned}$$

Thus, equations for R and T can be obtained as eqs(3.16)

$$0 = M_{21} + M_{22} R$$

$$R = \frac{-M_{21}}{M_{22}} \quad (3.16a)$$

$$\begin{aligned}
T e^{ik_c L} &= M_{11} + M_{12} R \\
&= M_{11} + M_{12} \left(-\frac{M_{21}}{M_{22}} \right)
\end{aligned}$$

$$|T| = \left| \frac{\det(M)}{M_{22}} \right| \quad (3.16b)$$

From the definition of \mathbf{M} , one can determine $\det(\mathbf{M})$ and M_{22} .

$$\begin{aligned} |\det \mathbf{M}| &= \frac{1}{2} \left(\frac{2\mu_c}{ik_c} \right) (\det \mathbf{S}) \left(\frac{2ik_e}{\mu_e} \right) \\ &= \frac{2\mu_c k_e}{\mu_e k_c} \end{aligned}$$

$$\mathbf{M} = \frac{1}{2} \begin{bmatrix} 1 & \frac{\mu_c}{ik_c} \\ 1 & \frac{-\mu_c}{ik_c} \end{bmatrix} \begin{bmatrix} S_{11} + S_{12} \frac{ik_e}{\mu_e} & S_{11} - S_{12} \frac{ik_e}{\mu_e} \\ S_{21} + S_{22} \frac{ik_e}{\mu_e} & S_{21} - S_{22} \frac{ik_e}{\mu_e} \end{bmatrix}$$

$$M_{22} = \frac{1}{2} \left\{ S_{11} - S_{12} \frac{ik_e}{\mu_e} - \frac{\mu_c}{ik_c} \left(S_{21} - S_{22} \frac{ik_e}{\mu_e} \right) \right\}$$

$$|M_{22}|^2 = \frac{1}{4} \left[\left(S_{11} + \frac{\mu_c k_e}{\mu_e k_c} S_{22} \right)^2 + \left(\frac{-k_e}{\mu_e} S_{12} + \frac{\mu_c}{k_c} S_{21} \right)^2 \right]$$

$$\begin{aligned} &= \frac{1}{4} \left[\left(S_{11}^2 + \frac{2\mu_c k_e}{\mu_e k_c} S_{11} S_{12} + \left(\frac{\mu_c k_e}{\mu_e k_c} \right)^2 S_{22}^2 + \left(\frac{k_e}{\mu_e} \right) S_{12}^2 \right. \right. \\ &\quad \left. \left. - \frac{2\mu_c k_e}{\mu_e k_c} S_{12} S_{21} + \left(\frac{\mu_c}{k_c} \right)^2 S_{21}^2 \right) \right] \end{aligned}$$

$$|M_{22}|^2 = \frac{\mu_c k_e}{4\mu_e k_c} \left[2 + \frac{\mu_e k_c}{\mu_c k_e} S_{11}^2 + \frac{k_c k_e}{\mu_c \mu_e} S_{12}^2 + \frac{\mu_c \mu_e}{k_c k_e} S_{21}^2 + \frac{\mu_c k_e}{\mu_e k_c} S_{22}^2 \right]$$

Therefore, the calculation of T_{tunnel} follows, and the result is eq(3.17)

$$T_{\text{tunnel}} = \frac{k_c \mu_e}{k_e \mu_c} \left(\frac{2 \mu_c k_e}{\mu_e k_c} \right)^2 \cdot \frac{1}{|M_{22}|^2}$$

$$T_{\text{tunnel}} = \frac{k_e \mu_c}{k_c \mu_e} \cdot \frac{4}{|M_{22}|^2}$$

$$T_{\text{tunnel}} = \frac{16}{2 + \frac{\mu_e k_c}{\mu_c k_e} S_{11}^2 + \frac{k_c k_e}{\mu_c \mu_e} S_{12}^2 + \frac{\mu_c \mu_e}{k_c k_e} S_{21}^2 + \frac{\mu_c k_e}{\mu_e k_c} S_{22}^2}$$

(3.17)

CHAPTER 4 THE APPLIED BIAS VOLTAGE

4.1 INTRODUCTION

The application of a bias voltage across a structure offers an obstacle to the model discussed in the previous chapters. This bias has the effect of tilting the band diagram while the model expects a piecewise flat band structure. The slope of a segment of the resulting band diagram depends on the dielectric constant of that layer. This problem is handled in section 4.2. The tilted band diagram is approximated by a staircase-like diagram in section 4.3. Here, a given superlattice and bias potential are used to generate a pseudo-structure that can be analyzed by the program. Thus, an applied bias can be included in the model. Section 4.4 explains the Fortran program in greater detail.

4.2 BIASING A LAYERED DIELECTRIC

4.2.1 Statement of the Problem

An elementary problem is the case of finding electric fields E and D in the dielectric layers of a capacitor. Figure 4.1 exemplifies the situation.

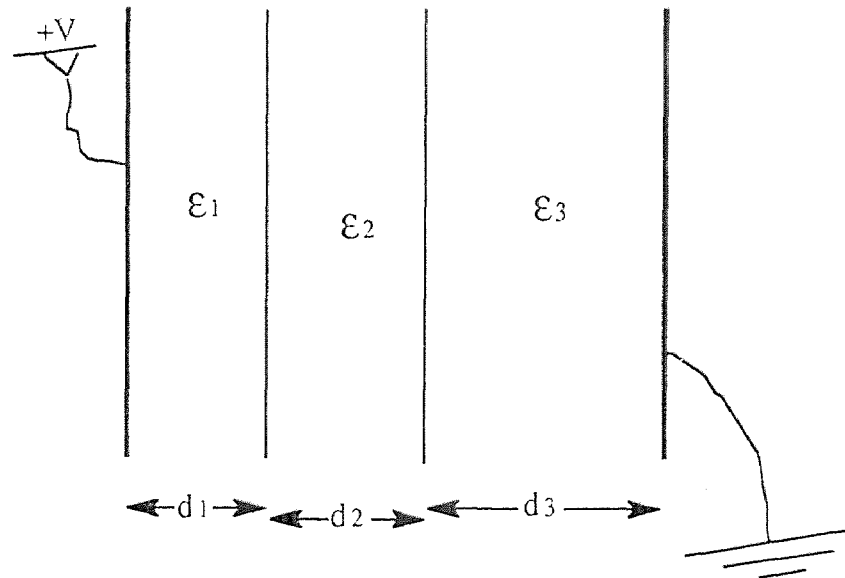


Figure 4.1 Biased Dielectric Layers

4.2.2 Solution to the Problem

This problem is solvable at sight. The normal component of D is continuous across the boundaries dividing the layers. Apply formula 4.1 along a path from left to right.

$$V = \int \mathbf{E} \cdot d\mathbf{l} \quad (4.1)$$

This means that $V = E_1 d_1 + \dots + E_3 d_3$. Therefore, in the i th layer,

$$E_i = \epsilon_0 \epsilon_i V \left(\frac{d_1}{\epsilon_1} + \dots + \frac{d_3}{\epsilon_3} \right)^{-1} \quad (4.2)$$

4.3 THE STEP APPROXIMATION

4.3.1 The Tilted Bands

It is clear from the previous section that an applied bias causes the bands to tilt. The slope of a segment of a band is essentially the electric field E in that layer. As was previously mentioned, this slope depends on the dielectric constants of the materials making up the superlattice. For the moment, assume the slope is the same for all layers. A possible band diagram is represented as figure 4.2, and the tilted band is depicted in figure 4.3.

Sample Band Diagram

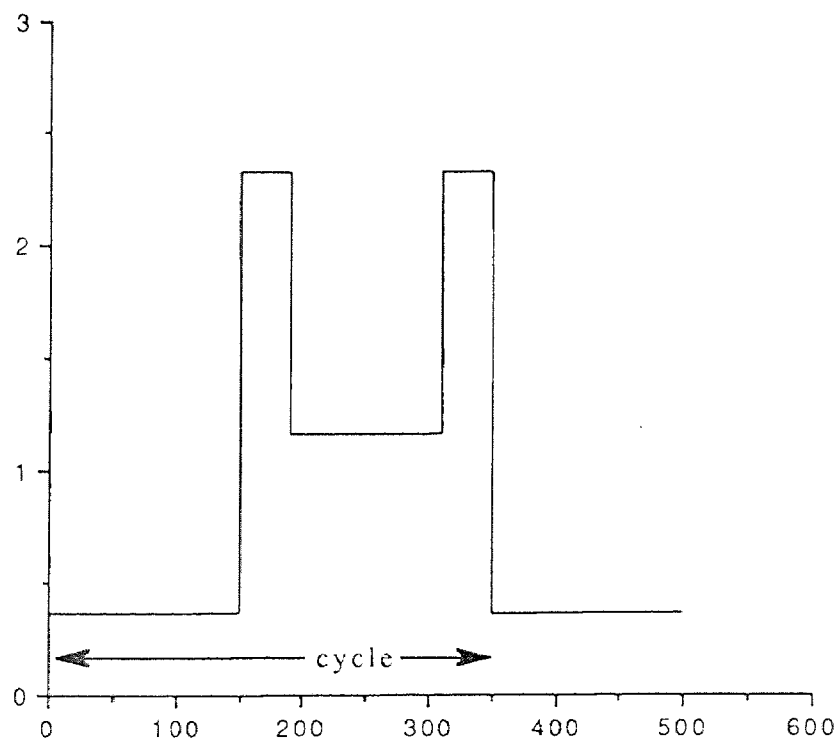


Figure 4.2 Sample Band Structure

Tilted Band Diagram

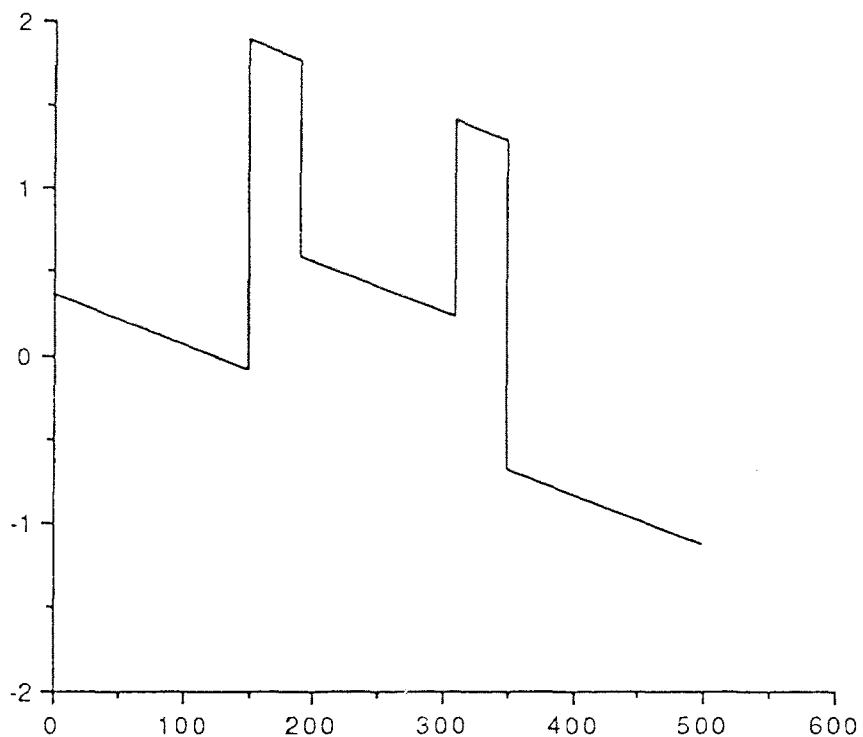


Figure 4.3 A Tilted Band

Notice that the last or fifth segment in the above diagrams is actually the beginning of the next cycle in the superlattice structure. The structure depicted above has a four-layered cycle. This will be important when the step approximation is applied to the tilted band.

4.3.2 The Step Approximation

The sloped band diagram is handled by a straightforward approximation. Each sloped segment is replaced by a number of steps as shown in figure 4.4. The result is a piecewise flat diagram that will be accepted by the computer program, and its accuracy increases with the number of steps.

Staircase Approximation

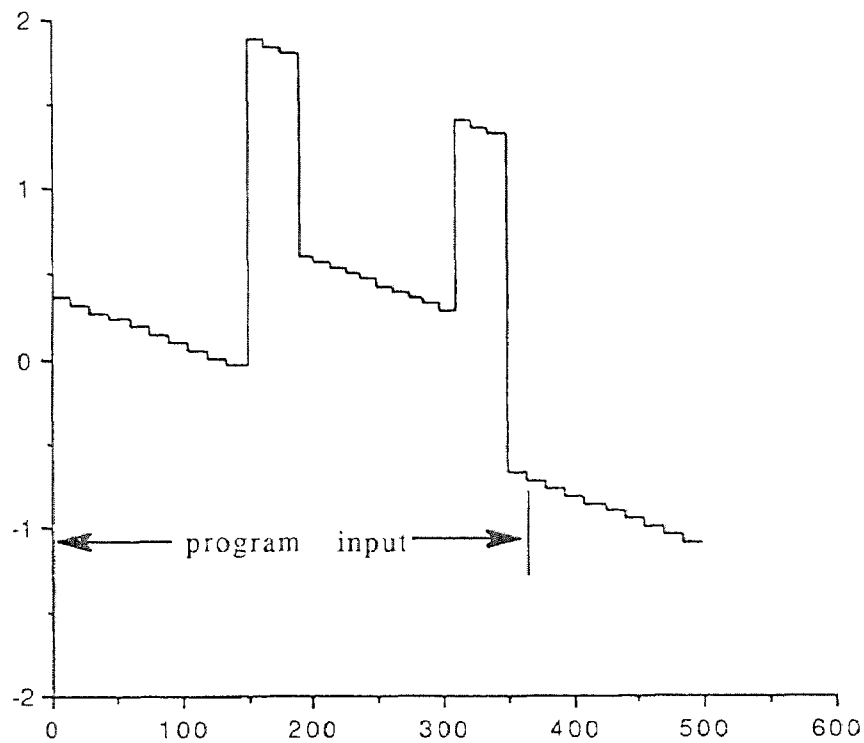


Figure 4.4 Steps Approximating a Tilted Band

4.4 THE FORTRAN PROGRAM

The program requires input describing a cycle of the structure plus one extra layer. This extra layer is the start of the next cycle. If, for instance, each of the five segments in figure 4.3 is broken into ten steps, then fifty steps would be pictured in figure 4.4. However, the "extra" layer that begins a new cycle in figure 4.4 is the forty first segment. Therefore the program input is indicated accordingly in that figure.

The program calculates subband structure and tunneling coefficients for a range of energies. Two input files are required. One describes the conduction and valence bands of the MQW. As was stated earlier, these effective parameters are assumed to be a priori known. The second input file needs to be constructed manually. It contains the slope of each segment of the band diagram and the number of steps used to approximate the sloped band. This information is calculated from an applied voltage, the dielectric constants of the constituent layers, and the thicknesses of the layers.

Several "self-consistency" tests were performed on the program. For a trial structure, the applied voltage was set to zero. The number of steps was varied from one to fifty with no difference in the output. Also, for an increasing, yet small, applied voltage, the results changed continuously from the unbiased case. Also, since it is required to supply one period to

the program, any layer can be considered as the first layer of the period. Indeed several possible ways were tried with no appreciable difference in output. If these tests yielded any other outcomes, then the model would have been rendered questionable.

The actual program and sample input and output files are included in the appendix.

CHAPTER 5

APPLYING THE SUPERLATTICE MODEL TO A DESIGN GOAL

5.1 INTRODUCTION

As a demonstration of the usefulness of the model discussed in the previous chapters, a design goal will be presented. The model will be applied to the design goal and used in the preliminary stages of the design process.

As the design objective, it is desired to develop a MQW infrared laser. Optical transitions between subbands in quantum well structures have received considerable attention[21-26]. The possibility of tuning the wavelength of the emission makes this objective important. Infrared lasing can occur utilizing a resonant tunneling diode structure[22], but this is subject to problems[21]. Several superlattice structures will be examined as to the feasibility of the desired goal.

The next section will discuss general considerations regarding population inversion, a fundamental condition for the realization of lasing. The remaining sections will apply the superlattice model to several structures and show how preliminary, numerical results can be of value.

5.2 GENERAL CONSIDERATIONS

Current injection by resonant tunneling has been proposed as a means of operating a possible lasing device. Current is injected into an upper subband of a MQW. The electrons can tunnel through the structure or move to a lower subband emitting radiation. Electrons in the lower subband tunnel through the device. Figure 5.1 shows this current injection scheme.

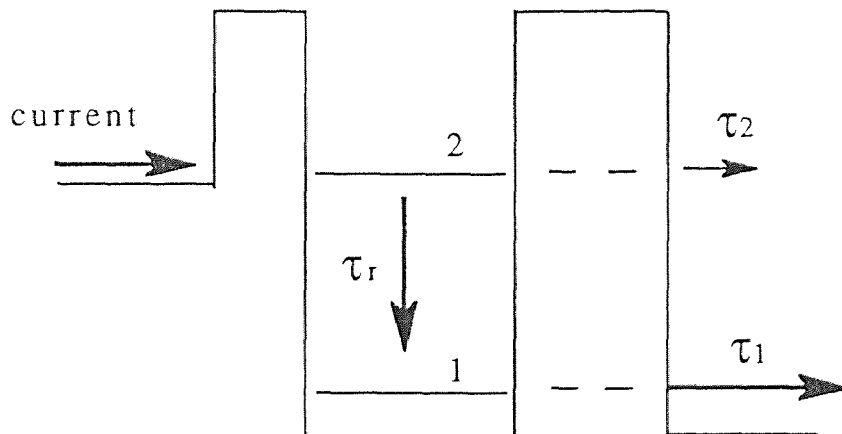


Figure 5.1 Current Injection Scheme

To have population inversion, the tunneling time through the upper level (2) should be greater than the relaxation time to the lower level (2 to 1). In addition this relaxation time should be greater than the lower level (1) tunneling time.

$$\tau_2 > \tau_r > \tau_1 \quad (5.1)$$

5.3 PRELIMINARY STRUCTURE

One possible design is a diode-like structure composed of type-II heterojunctions[24]. Recent tunneling measurements in such structures have shown negative differential resistance[16,17,19]. Figure 5.2 shows a structure under a small bias and approximated by steps as discussed in chapter 4.

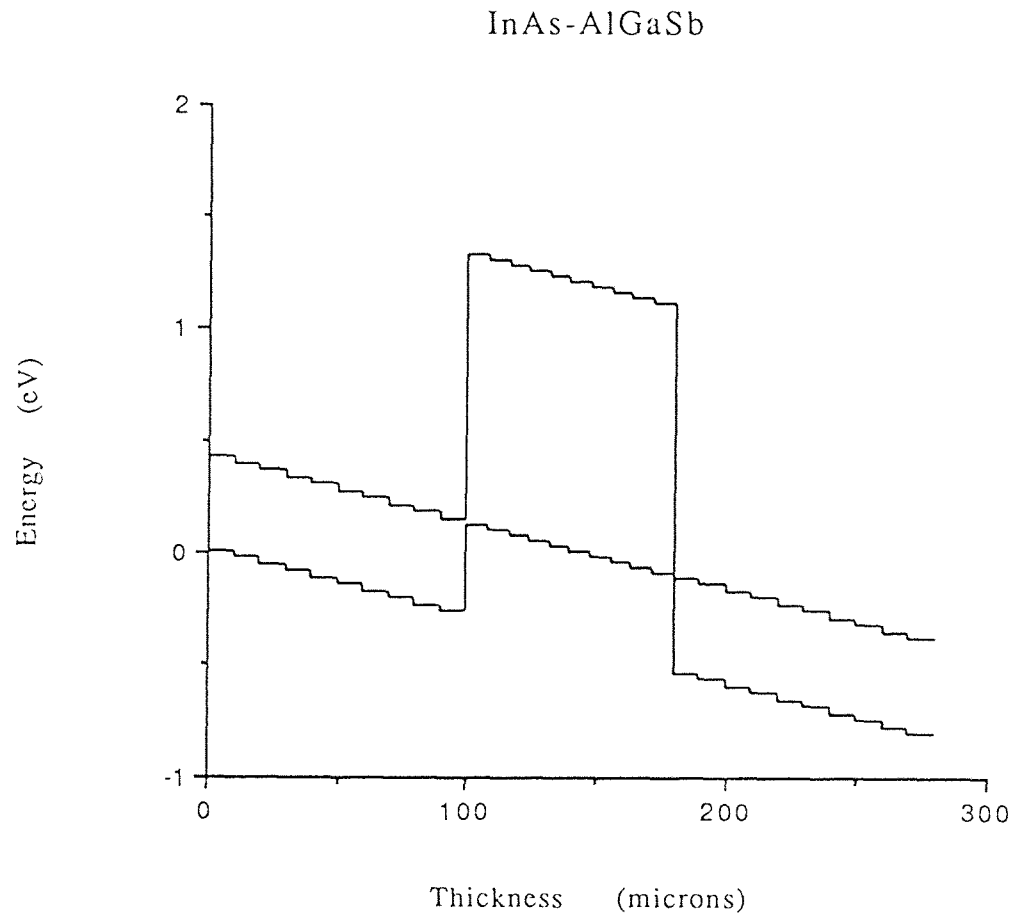


Figure 5.2 Structure 1

The calculated tunneling characteristics are shown in figure 5.3

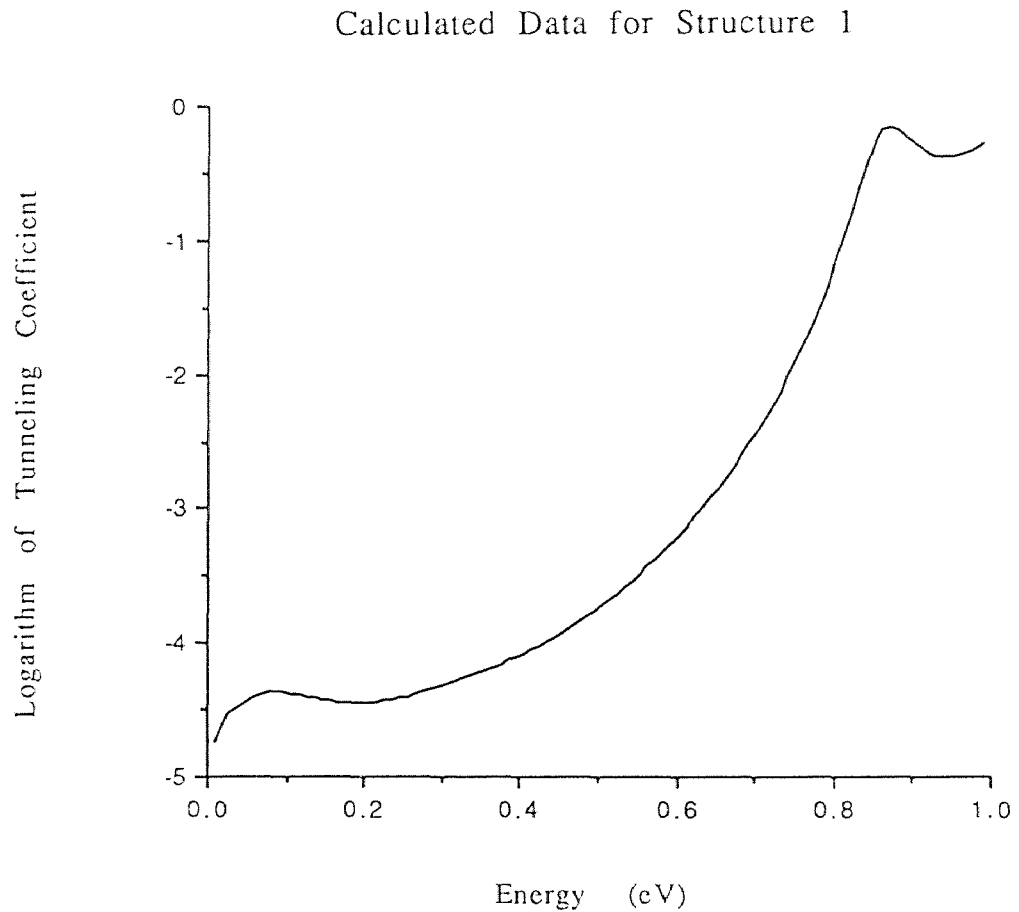


Figure 5.3 Tunneling Data for Structure 1

This data does not satisfy eq(5.1). Population inversion is not achieved. Varying the thickness of the barrier gave similar results

As another attempt consider structure 2 in figure 5.4. Two barriers of different thicknesses make up this structure.

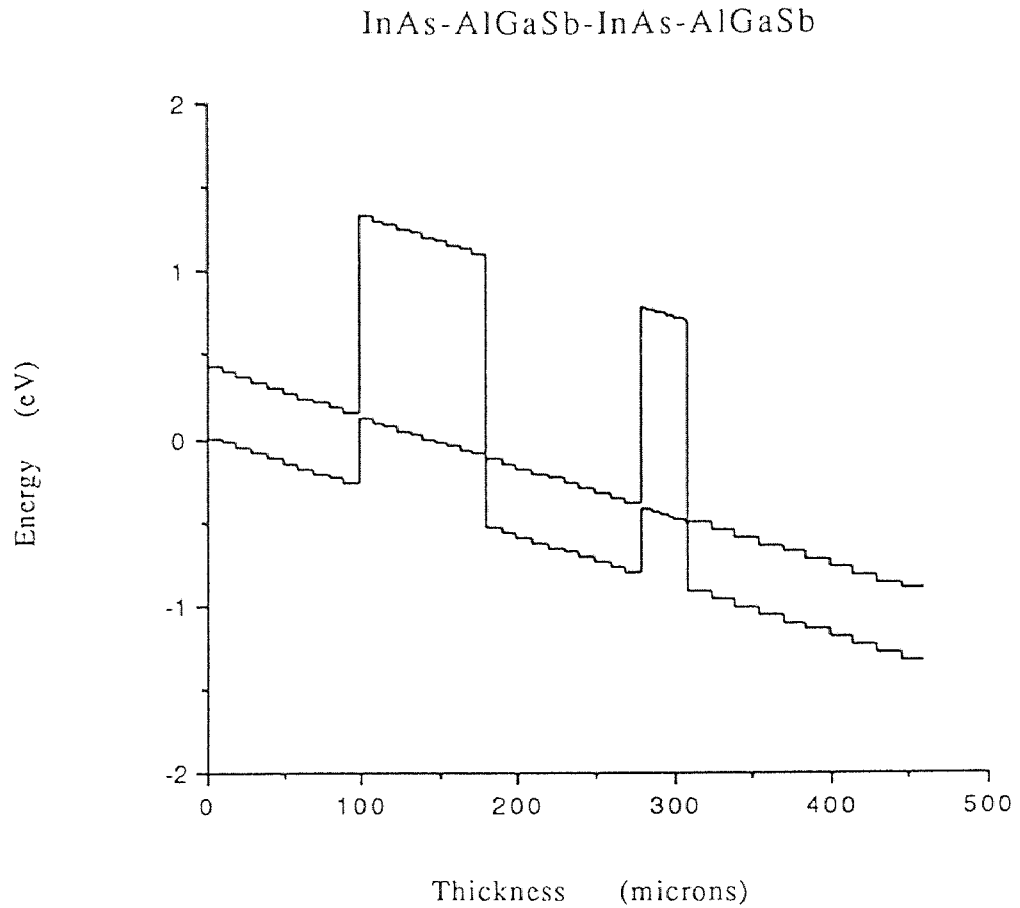


Figure 5.4 Structure 2

The tunneling data is presented as figure 5.5. This data shows promise. The negative slope of portions of the tunneling data shows the possibility of population inversion. However the effect needs to be enhanced.

Calculated Data for Biased Structure 2

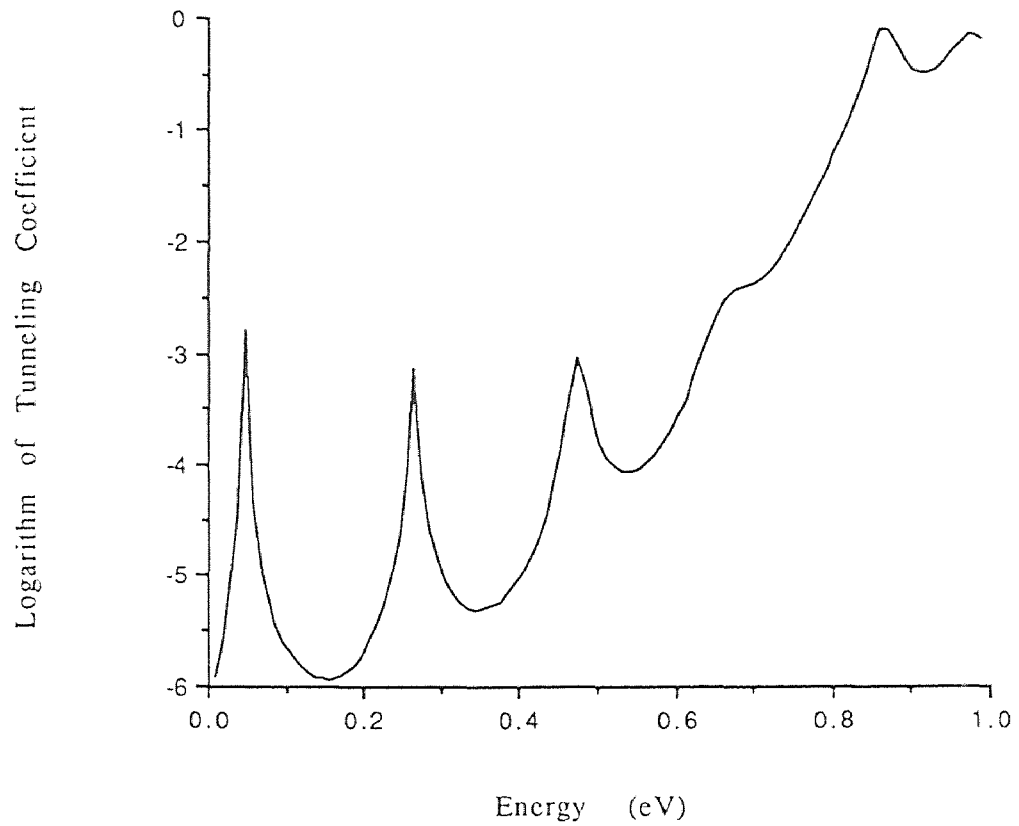


Figure 5.5 Data for structure 2

Another possibility is structure 3 shown in figure 5.6 [16-20,27]. In this structure, the upper subband in the InAs well is blocked by the forbidden gap of GaSb. The lower subband in the well can tunnel through the valence band of GaSb. The AlSb layers enhance the effect.

InAs-AlSb-GaSb-AlSb

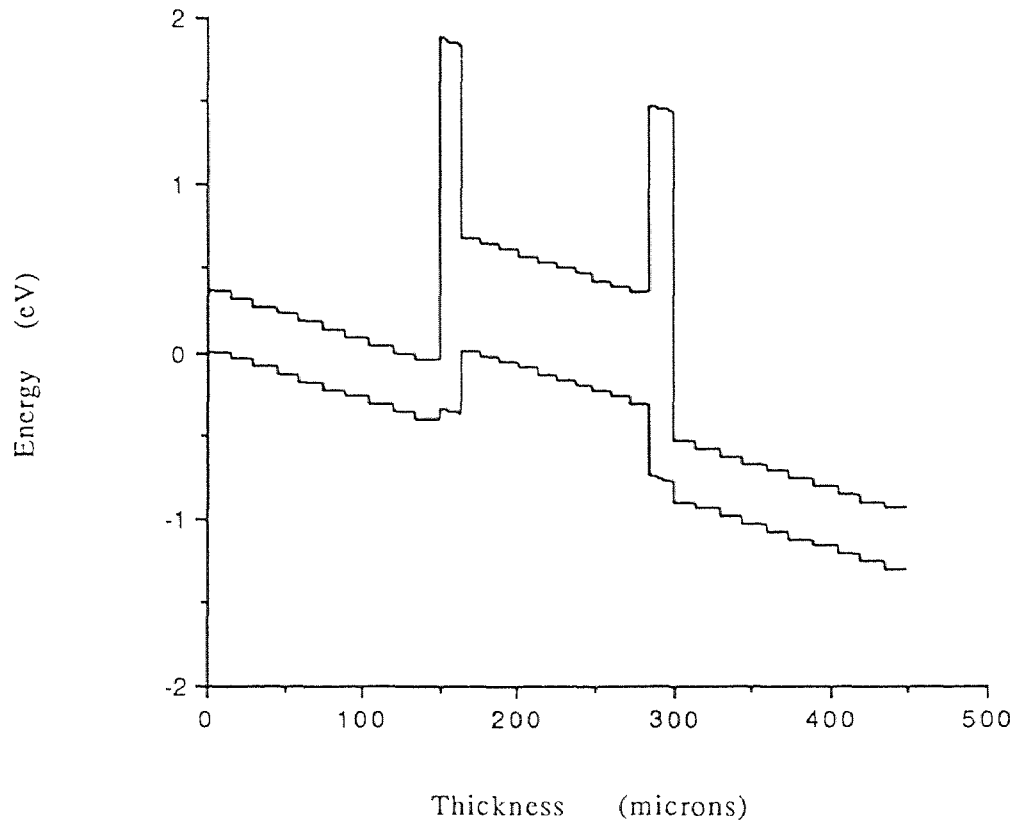


Figure 5.6 Structure 3

The tunneling data is presented in figure 5.7. This data shows enhanced results over structure 2. The peaks in the data occur close to unity while a sufficient negative slope is achieved. It remains to fine tune the data by varying thicknesses and perhaps trying different materials.

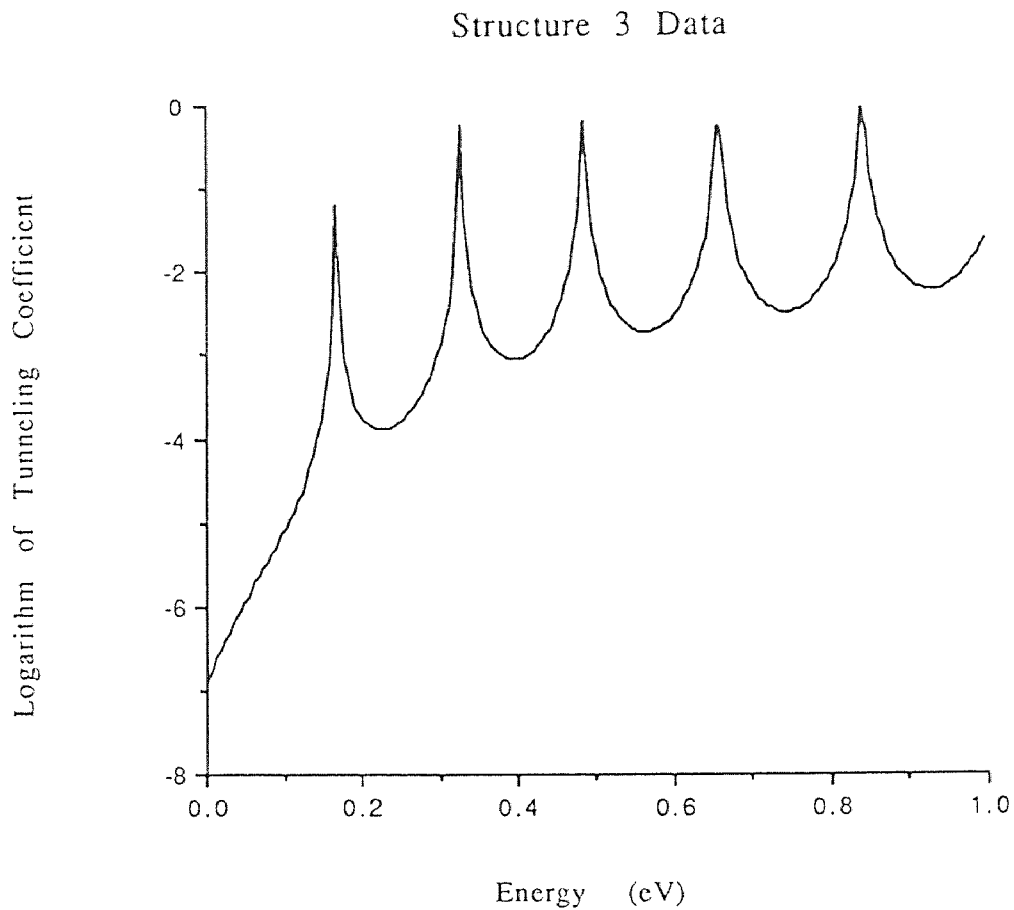


Figure 5.7 Data for Structure 3

It is clear that this model with program makes preliminary calculations on many different structures possible. Such a model can save a designer time in the early stages of development. The goal of this work was to present the model as a design tool. Of course any design objective requires exhaustive use of many resources, and this model is offered as one.

APPENDIX

A.1 INTRODUCTION

For the sake of completeness, relevant input and output files, along with the Fortran-77 program are included here. Figure A.1 shows the relationships among these files. Subsequent sections of this appendix include brief descriptions and samples of the files.

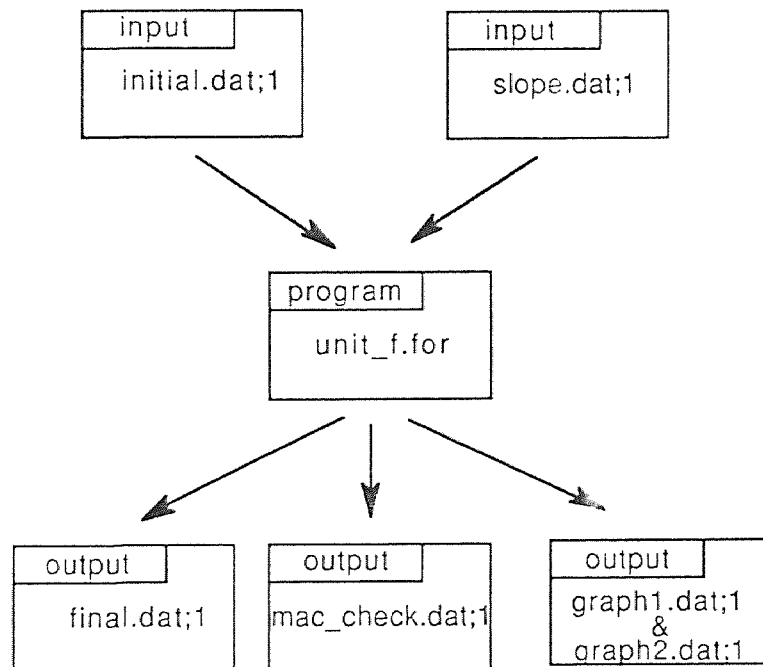


Figure A.1 Pictorial representation of computer files

A.2 INPUT FILES

Two input files are accessed by the Fortran-77 program. The first is called 'initial.dat;1'. It consists of seven lines. The first line contains the coupling parameter. Next is the number of materials in a period (plus one). The last five lines describe the energy band diagram. Each line contains a width, an energy gap, and the conduction band offset related to the first layer. A sample file follows and is represented in figure A.2

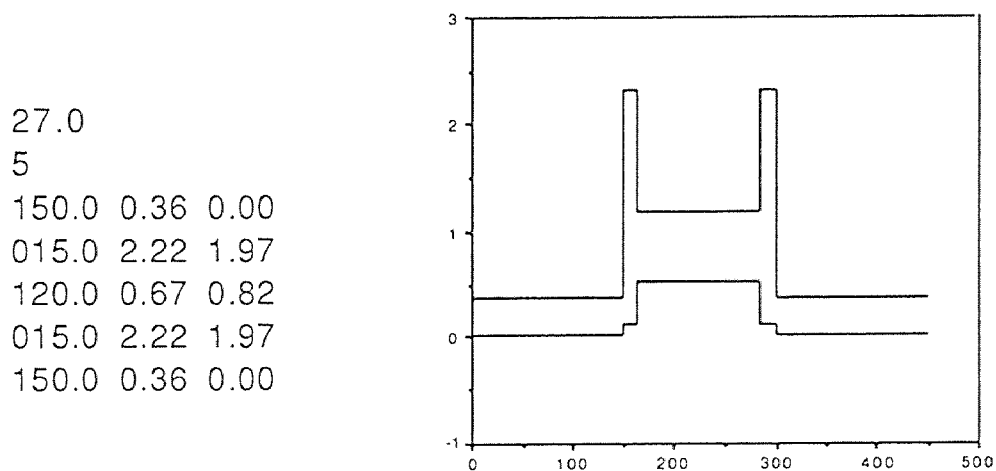


Figure A.2 Sample input file 'initial.dat;1' and graphical representation

The second input file is called 'slope.dat;1'. It contains the number of energy steps or increments on the first line. Next comes the energy range over which the program studies the structure. Each subsequent line contains a slope of the energy band diagram for a layer and the number of flat steps used to approximate the biased layer. The listing follows in figure A.3 along with a graph showing how the biased structure is approximated.

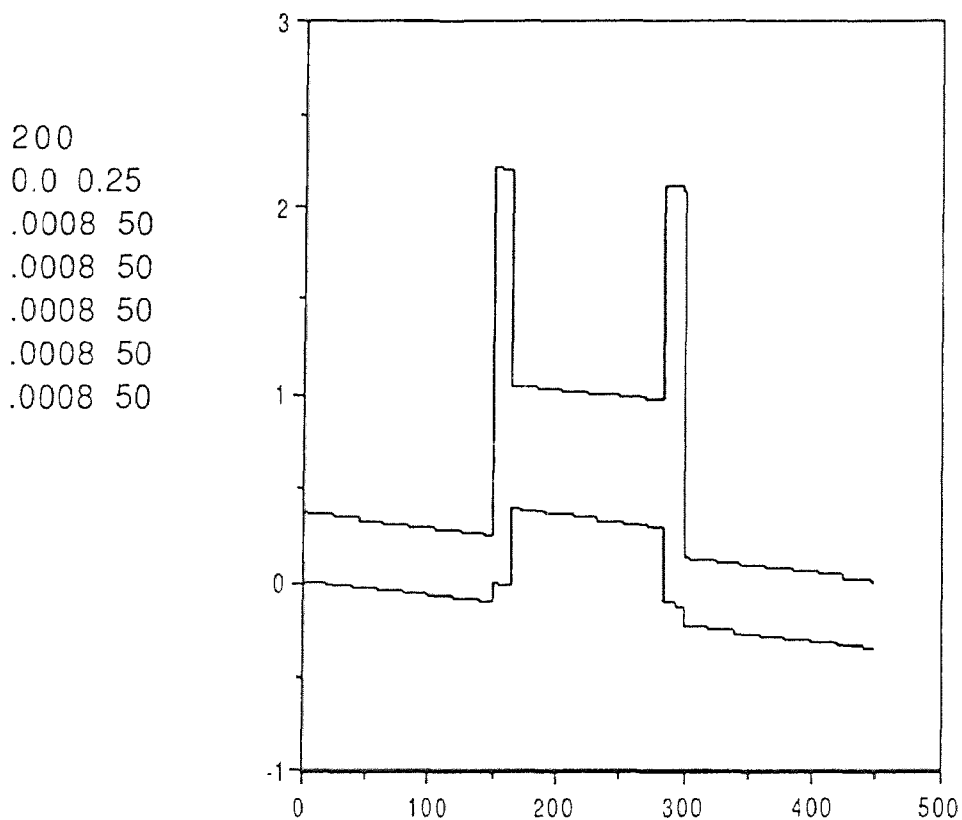


Figure A.3 Sample input file 'slope.dat;1' and graph of the step approximation

A.3 FORTRAN-77 PROGRAM

The following Fortran-77 program calculates subband structure, tunneling coefficients, and other data. This program ran under VAX/VMS.

```

real*8 iw(10),ieg(10),ivs(10),sl(10)
real*8 px(100),py(100),x(10),y(10)
real*8 w(300),eg(300),vs(300)
real*8 a,cp,e0,em,estep,e,o,u
real*8 z1(300),z2(300),z3(300)
real*8 s11,s12,s21,s22,t11,t12,t21,t22
real*8 h11,h12,h21,h22,h1,h3,q,r,t,lgt,temp
real*8 a1,a2,a3,a4
real g(300)
integer ibr(10)
character elevel*7
data a/0.26246644d0/
data o/0.0d0/
data u/1.0d0/
open(2,file='initial.dat;l',status='old')
rewind(2)
open(6,file='slope.dat;l',status='old')
rewind(6)
read(2,*)cp
read(2,*)n1
read(6,*)ntot
read(6,*)e0,em
do 280 i=1,n1
read(2,*)iw(i),ieg(i),ivs(i)
280 continue
close(2)
x(1)=0.0d0
y(1)=ieg(1)

```

```

read(6,*)sl(1),ibr(1)
n=ibr(1)
call pieces(x(1),y(1),iw(1),ibr(1),sl(1),px,py)
open(7,file='mac_check.dat;l',status='new')
do 333 i=1,ibr(1)
eg(i)=ieg(1)
w(i)=iw(1)/ibr(1)
vs(i)=py(i)-y(1)
101  format(1x,3f16.8)
q1=real(px(i))
q2=real(py(i))
q3=real(py(i)-eg(1))
write(7,101)q1,q2,q3
333  continue
temp=0.0d0
do 300 i=2,n1
read(6,*)sl(i),ibr(i)
temp=temp+sl(i-1)*iw(i-1)
x(i)=x(i-1)+iw(i-1)
y(i)=y(1)+ivs(i)-temp
call pieces(x(i),y(i),iw(i),ibr(i),sl(i),px,py)
do 334 j=n+1,n+ibr(i)
eg(j)=ieg(i)
w(j)=iw(i)/ibr(i)
vs(j)=py(j-n)-y(1)
q1=real(px(j-n))
q2=real(py(j-n))
q3=real(py(j-n)-eg(j))
write(7,101)q1,q2,q3
334  continue
n=n+ibr(i)
300  continue
close(6)
close(7)
n=n+1-ibr(n1)
estep=(em-e0)/(ntot+1.0d0)

```



```

e=e0
open(3,file='final.dat;1',status='new')
rewind(3)
do 281 i=1,ntot
e=e+estep
do 282 j=1,n
z1(j)=1.5d0*(e+eg(j)-vs(j))/cp
z2(j)=a*z1(j)*(e-vs(j))
z3(j)=dsqrt(dabs(z2(j)))
282  continue
s11=1.0d0
s12=0.0d0
s21=0.0d0
s22=1.0d0
do 283 j=2,n-1
if (z2(j).lt.0.0d0) then
call work1(t11,t22,t12,t21,z3(j),w(j),o,u,z1(j))
else
call work1(t11,t22,t12,t21,z3(j),w(j),u,o,z1(j))
endif
call work2(t11,t12,t21,t22,s11,s12,s21,s22)
283  continue
call work1(h11,h22,h12,h21,z3(1),w(1),u,o,z1(1))
q=(h11*s11+h22*s22+h12*s21+h21*s12)/2.0d0
r=dabs(q)
elevel='subband'
if (r.gt.1.0d0) elevel='      '
h1=z3(n)/z1(n)*z1(1)/z3(1)
h3=z3(n)/z1(n)*z3(1)/z1(1)
a1=h1*s11*s11
a2=s22*s22/h1
a3=h3*s12*s12
a4=s21*s21/h3
t=4.0d0/(2.0d0+a1+a2+a3+a4)
lgt=dlog10(t)
g(i)=lgt

```

```

284   format(1x,3d16.8,a7,d16.8)
      write(3,284)t,lgt,e,elevel,q
281   continue
      close(3)
      call graph1(g,0.0,ntot)
      call graph2(g,ntot)
      end
      subroutine work1(a1,a2,a3,a4,b,c,d,e,f)
      real*8  a1,a2,a3,a4,b,c,d,e,f
      a1=d*dcos(b*c)+e*dcosh(b*c)
      a2=a1
      a3=d*f/b*dsin(b*c)+e*f/b*dsinh(b*c)
      a4=-1.0*d*b/f*dsin(b*c)+e*b/f*dsinh(b*c)
      return
      end
      subroutine work2(t11,t12,t21,t22,s11,s12,s21,s22)
      real*8  s11,s12,s21,s22,t11,t12,t21,t22,a,b,c,d
      a=t11*s11+t12*s21
      b=t11*s12+t12*s22
      c=t21*s11+t22*s21
      d=t21*s12+t22*s22
      s11=a
      s12=b
      s21=c
      s22=d
      return
      end
      subroutine pieces(x,y,w,n,m,px,py)
      real*8  x,y,w,px(100),py(100),m,c
      c=w/n
      px(1)=x
      py(1)=y
      do 99 j=2,n
      px(j)=px(j-1)+c
      py(j)=py(j-1)-m*c
99   continue

```

```

return
end
subroutine graph1(y,tol,ntot)
real y(300)
open(9,file='graph1.dat;1',status='new')
rewind(9)
a=y(1)
b=y(2)
do 173 j=1,ntot
if (y(j).lt.a) a=y(j)
if (y(j).gt.b) b=y(j)
173  continue
c=b-a
if (c.lt.tol) then
write(9,*)'no graph'
return
else
do 174 i=1,ntot
j=int((y(i)-a)/c*70+1)
write(9,*)(' ',k=1,j),'*'
174  continue
endif
close(9)
return
end
subroutine graph2(g,ntot)
real g(300)
character*1 x(300),y(100)
open(8,file='graph2.dat;1',status='new')
rewind(8)
DO 1010 J=1,71
1010  Y(J)='- '
DO 1020 J=1,8
J1=10*J-9
1020  Y(J1)='+'
WRITE(8,*)(Y(J),J=1,71)

```

```
DO 1070 I=1,ntot
  IF (MOD(I,10).EQ.0) GOTO 1040
  X(1)='l'
  X(71)='l'
  GOTO 1050
1040  X(1)='+ '
      X(71)='+ '
1050  DO 1060 J=2,70
1060  X(J)=' '
      I1=INT(71+10*G(I)+0.5)
      IF (I1.LT.1) I1=1
      X(I1)='*'
      WRITE(8,*) (X(J),J=1,71)
1070  CONTINUE
      WRITE(8,*) (Y(J),J=1,71)
      close(8)
      return
      end
```

A.4 Output Files

Four output files are generated by the Fortran-77 program. The most important is called 'final.dat;l'. It contains columns showing tunneling coefficient, log of tunneling coefficient energy, and subband indicator. A sample file is listed below.

1.907E-01	-7.196E-01	5.000E-03		2.211E+00
3.656E-01	-4.370E-01	1.000E-02	subband	-8.943E-01
7.814E-02	-1.107E+00	1.500E-02		-3.364E+00
3.738E-02	-1.427E+00	2.000E-02		-5.172E+00
2.353E-02	-1.628E+00	2.500E-02		-6.317E+00
1.695E-02	-1.771E+00	3.000E-02		-6.821E+00
1.326E-02	-1.877E+00	3.500E-02		-6.726E+00
1.099E-02	-1.959E+00	4.000E-02		-6.096E+00
9.518E-03	-2.021E+00	4.500E-02		-5.014E+00
8.560E-03	-2.068E+00	5.000E-02		-3.578E+00
7.960E-03	-2.099E+00	5.500E-02		-1.899E+00
7.643E-03	-2.117E+00	6.000E-02	subband	-9.532E-02
7.580E-03	-2.120E+00	6.500E-02		1.709E+00
7.779E-03	-2.109E+00	7.000E-02		3.390E+00
8.297E-03	-2.081E+00	7.500E-02		4.831E+00
9.258E-03	-2.033E+00	8.000E-02		5.922E+00
1.093E-02	-1.961E+00	8.500E-02		6.568E+00
1.391E-02	-1.857E+00	9.000E-02		6.694E+00
1.972E-02	-1.705E+00	9.500E-02		6.245E+00
3.333E-02	-1.477E+00	1.000E-01		5.193E+00
7.928E-02	-1.101E+00	1.050E-01		3.537E+00
4.525E-01	-3.444E-01	1.100E-01		1.309E+00
2.925E-01	-5.339E-01	1.150E-01		-1.430E+00
4.559E-02	-1.341E+00	1.200E-01		-4.587E+00
1.547E-02	-1.810E+00	1.250E-01		-8.039E+00
7.158E-03	-2.145E+00	1.300E-01		-1.163E+01
3.895E-03	-2.410E+00	1.350E-01		-1.519E+01
2.342E-03	-2.630E+00	1.400E-01		-1.851E+01
1.508E-03	-2.821E+00	1.450E-01		-2.138E+01
1.021E-03	-2.991E+00	1.500E-01		-2.357E+01
7.182E-04	-3.144E+00	1.550E-01		-2.484E+01
5.207E-04	-3.283E+00	1.600E-01		-2.496E+01
3.871E-04	-3.412E+00	1.650E-01		-2.371E+01
2.938E-04	-3.532E+00	1.700E-01		-2.087E+01
2.270E-04	-3.644E+00	1.750E-01		-1.627E+01
1.781E-04	-3.749E+00	1.800E-01		-9.759E+00

Another output file is called 'mac_check.dat;1'. This file contains x and y coordinates of points defining the step approximation to the biased structure. It is used to generate pictures like figure A.3 and is not reproduced here. Finally, two preliminary graphs are produced by the program, 'graph1.dat;1', and 'graph2.dat;1'. The author found it convenient to see preliminary results graphically. Figure A.4 shows a sample.

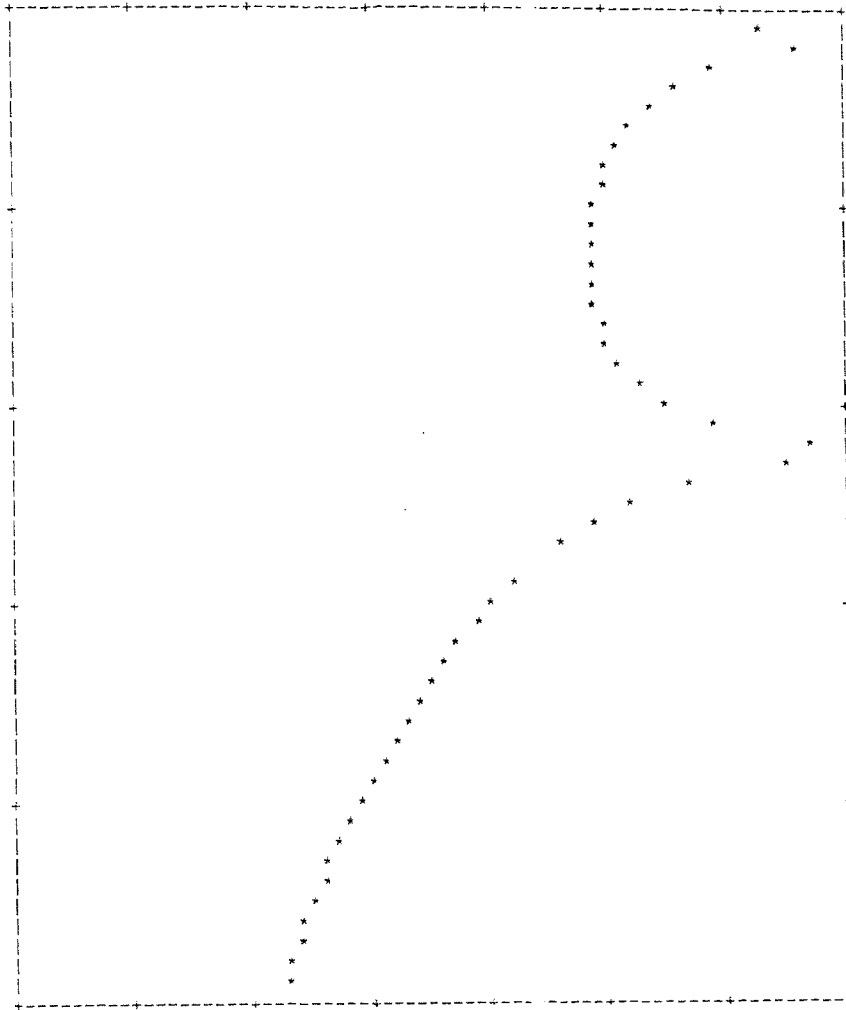


Figure A.4 Preliminary graph produced by program

BIBLIOGRAPHY

- [1] Kane, E. O. "Band Structure of Indium Antimonide." *J. Phys. Chem. Solid* 1 (1957): 249-261.
- [2] Tsu, R., and L. Esaki. "Tunneling in a Finite Superlattice." *Appl. Phys. Lett.* 22 (1973): 562-564.
- [3] Esaki, L. "A Bird's-Eye View on the Evolution of Semiconductor Superlattice and Quantum Wells." *IEEE QE-22* (1986): 1611-1624.
- [4] Bastard, G. "Theoretical Investigations of Superlattice Band Structure in the Envelope Function Approximation." *Phys. Rev. B* 25 (1982): 7584-7597.
- [5] Bastard, G., and J. A. Brum. "Electronic States in Semiconductor Heterostructures." *IEEE QE-22* (1986): 1625-1644.
- [6] Altarelli, M. "Electronic Structure and Semiconductor-Semimetal Transition in InAs-GaSb Superlattices." *Phys. Rev. B* 28 (1983): 842-845.
- [7] Cho, H. S., and P. R. Pruncnal. "New Formalism of the Kronig-Penney Model with Application to Superlattices." *Phys. Rev. B* 36 (1987): 3237-3242.
- [8] Schuurmans, M. F. H., and G. W. t'Hooft. "Simple Calculations of Confinement States in a Quantum Well." *Phys. Rev. B* 31 (1984): 88047.
- [9] Wang, K. L., and P. F. Yu. "Theory and Applications of Band-Aligned Superlattices." *IEEE QE-25* (1989): 12-19.

- [10] Cuypers, T. P., and W. Van Haeringen. "On the Theory of Envelope Function in Lattice-Matched Heterostructures." *Physica B* 168 (1990): 58-66.
- [11] Hickmott, T. W., and P. M. Solomon. "Negative Charge, Barrier Heights, and the Conduction-Band Discontinuity in $\text{Al}_x\text{Ga}_{1-x}\text{As}$ Capacitors." *J. Appl. Phys.* 57 (1984): 2844-2853.
- [12] Dawson, P., B. A. Wilson, C.W. Tu, and R. C. Miller. "Staggered Band Alignments in AlGaAs Heterojunctions and the Determination of Valence-Band Offsets." *Appl. Phys. Lett.* 48 (1986): 541-543.
- [13] Wang, W. I., E. E. Mendez, and F. Stern. "High Mobility Hole Gas and Valence-Band in Modulation-Doped p-AlGaAs/GaAs Heterojunctions." *Appl. Phys. Lett.* 45 (1984): 639-640.
- [14] Jogai, B., and K. L. Wang. "Dependence of Tunneling Current of Structural Variations of Superlattice Devices." *Appl. Phys. Lett.* 46 (1984): 167-168.
- [15] Gerard, J. M., and J. Y. Marzin. "Direct Probing of Type-II Band Configurations in Semiconductor Superlattices." *Phys. Rev. B* 40 (1988): 6450-6453.
- [16] Beresford, R., L. F. Luo, and W. I. Wang. "Negative Differential Resistance in AlGaSb/InAs Single-Barrier Heterostructures at Room Temperature." *Appl. Phys. Lett.* 54 (1989): 2023-2025.

- [17] Soderstrom, J. R., D. H. Chow, and T. C. McGill.
"Demonstration of Large Peak-to-Valley Current Ratios in InAs/AlGaSb/InAs Single-Barrier Heterostructures." *Appl. Phys. Lett.* 55 (1989): 1348-1350.
- [18] Hermans, J., D. L. Partin, and P. D. Dresselhaus.
"Tunneling through Narrow-Gap Semiconductor Barriers." *Appl. Phys. Lett.* 48 (1986): 644-646.
- [19] Miles, R. H., D. H. Chow, J. N. Schulman, and T. C. McGill.
"Infrared Optical Characterization of InAs/Ga_{1-x}Al_xSb Superlattices." *Appl. Phys. Lett.* 57 (1990): 801-803.
- [20] Sweeny, M., and J. M. Xu. "Resonant Interband Tunnel Diodes." *Appl. Phys. Lett.* 54 (1988): 546-548.
- [21] Helm, M., P. England, E. Colas, F. DeRosa, and S. J. Allen.
"Intersubband Emission from Semiconductor Superlattices Excited by Sequential Resonant Tunneling." *Phys. Rev. Lett.* 63 (1989): 74-79.
- [22] Kastalsky, A., V. J. Goldman, and J. H. Abeles.
"Magnetic Field-Induced Suppression of Acoustic Phonon Emission in a Superlattice." *Appl. Phys. Lett.* 59 (1991): 2636-2638.
- [23] Yang, R. Q., and J. M. Xu. "Population Inversion through Resonant Interband Tunneling." *Appl. Phys. Lett.* 59 (1991): 181-182.
- [24] Helm, M., and S. J. Allen. "Can Barriers with Inverted Tunneling Rates Lead to Subband Population Inversion?" *Appl. Phys. Lett.* 56 (1990): 1366-1368.

- [25] Borenstain, S., and J. Katz. "Intersubband Auger Recombination and Population Inversion in Quantum-Well Subbands." *Phys. Rev. B* 39 (1989): 10852-10857.
- [26] Kastalsky, A., and A. L. Efros. "Possibility of Infrared Laser in a Resonant Tunneling Structure." *J. Appl. Phys.* 69 (1991): 841-845.
- [27] Sai-Halasz, G. A., L. Esaki, and W. A. Harrison. "InAs-GaSb Superlattice Energy Structure and its Semiconductor-Semimetal Transition." *Phys. Rev. B* (1978): 2812-2818.
- [28] Bauerle, R. T., T. Elsaesser, W. Kaiser, H. Lobentanzer, W. Stolz, and K. Ploog. "Picosecond Infrared Spectroscopy of Hot Carriers in a Modulation-Doped Ga_{0.47}In_{0.53}As Multiple-Quantum-Well Structure." *Phys. Rev. B* 38 (1988): 4307-4310.
- [29] Vassell, M. O., J. Lee, and H. F. Lockwood. "Multibarrier Tunneling in Ga_{1-x}Al_xAs/GaAs Heterostructures." *J. Appl. Phys.* 54 (1983): 5206-5213.
- [30] Swisher, G. M. "Introduction to Linear Systems Analysis." Wiley, New York (1985): 350-437.
- [31] Chen, Hong "A Theoretical Study of the Subband Structures & Tunneling in Polytype Heterostructures" A thesis submitted to the faculty of New Jersey Institute of Technology 1992